



C/C MATERIAL DENSIFICATION BY CVI PROCESS: FROM EXPERIMENTAL TO SIMULATING RESULTS

J. Raynaud¹, Y. Quiring², C. Cairey Remonay², G. Borne¹, V. Bontempi¹, E. Schaer², R. Fournet²

Abstract

R-CVI (rapid chemical vapor infiltration) allows producing ceramic matrix composite material and more specifically carbon/carbon materials with good mechanical properties at high temperature. A numerical simulation model has been developed to understand and improve r-CVI process. The simulation model seems to give good qualitative and to a lesser extent quantitative result in comparison with experimental results. Finally, a parametric simulation study suggests ways of improving the process.

Keywords: *r-CVI, CMC, C/C, simulation*

1. Introduction

Ceramic Matrix Composites (CMCs) and more specifically Carbon/Carbon (C/C) materials have emerged in the high-technology field of aerospace, for instance for rocket boosters or aircraft brakes due to high temperature resistance and lightness[1]. These high-performance materials have several advantages as excellent mechanical properties at high temperature, low density and small thermal expansion [2]. In order to produce C/C materials, Chemical Vapor Infiltration (CVI) is a widely used technique [3], [4]. CVI is a chemical process based on hydrocarbon cracking to create pyrocarbon (PyC) precursors that are deposited in a porous preform. This pyrocarbon will be the matrix of the CMC whereas the porous preform is reinforced. There are several types of CVI but this study focuses on 2 interesting techniques:

- I-CVI, involving constant pressure and temperature. This technique is fairly simple to implement and produces good properties for the final product. It is the most widely used in industrial environments, but production cycles are very long (several weeks).
- r-CVI requires higher gas flow rates, temperature and pressure than conventional I-CVI [5]. As I-CVI, the process is isothermal and isobaric. The key advantages of this technique are reduced cycle times, reduced residual porosity and controlled gas flow, but specific tooling must be created for each material to be reinforced.

The objectives of this paper are the simulation of the various phenomena involved in densification, in order to optimize this process. These simulations are performed using COMSOL Multiphysics, and include multidisciplinary processes, combining chemistry, gas flow and heat transfer. 2D or 3D simulations should help improve matrix homogeneity, with the aim of controlling the impact of gas flow, heating and process parameters on chemistry and deposition. The development of this model requires comparisons between experimental and simulation data, in order to validate it. Some results of the comparison will be presented below.

2. Methodology and numerical setup

2.1. Chemical model adaptations

To begin this work, a homogeneous chemical model of propane pyrolysis which contains methane reactions was previously developed by Ziegler et al. [6], [7] and then adapted to our experimental densification conditions. This detailed model has been reduced using flow rate and sensitivity analysis.

¹ MBDA, France

² LRGP, 1 Rue Grandville, 54000 Nancy, France

The model changes from 189 species and 600 reactions to 10 species (C_2H_2 , C_2H_3 , C_2H_4 , C_2H_5 , C_2H_6 , CH_4 , CH_3 , H_2 , H , N_2) and 28 chemical reactions. This reduced model is able to reproduce the pyrolysis of methane under our operating. Moreover, the reduced mechanism generated allows preserving calculation resources (time and RAM) and can be combined with thermal and gas flow models.

Homogeneous model is not sufficient to describe carbon deposition. Another heterogeneous model, based on a previous study developed by Lacroix et al. [8] for propane pyrolysis to describe the transition between gas and solid phases has been added. In order to couple chemistry with flow and heat transfer, the heterogeneous model has been reduced. The technic was different from homogeneous one. Gas precursors of PyC have been identified (CH_3 , C_2H_2 and C_2H_4) and an Arrhenius law has been written for these 3 species as a function of the deposition rate. This simplification globalizes all elementary surface reactions. Then, the part of each reactant on the deposition has been quantified. Equation 1 shows the deposition law which is finally used in simulations with α , β , γ being parts of each species in the deposition, $k_{C_2H_2}$, $k_{C_2H_4}$, k_{CH_3} are global rate constants of precursors, $[C_2H_2]$, $[C_2H_4]$, $[CH_3]$ the concentrations of species and K a correction factor which was fitted to reproduce experimental results.

$$\begin{cases} r_{dep} = (2 \times \alpha \times k_{C_2H_2} \times [C_2H_2] + 2 \times \beta \times k_{C_2H_4} \times [C_2H_4] + \gamma \times k_{CH_3} \times [CH_3]) \times K \\ \alpha + \beta + \gamma = 1 \end{cases}$$

Equation 1

The following part details the coupling between chemistry, fluid flow and thermal transfer.

2.2. Fluid flow and thermal modeling

The reactor is composed of 3 parts: the gas injection chamber, the reacting part where densification proceeds, and another specific device for gas outlet. In the gas injection part, where velocities are the highest, the Mach number is equal to 0.4 and the Reynold number is equal to 1100. This allows simplifying fluid flow equations in the whole reactor as laminar compressible (Navier-Stocks equations). Concerning the modeling of the heat transfer phenomena, the oven is about 1400 K so the radiation has to be considered for solid/solid interactions. Concerning fluid and solid exchanges. Most heat transfer takes place by convection at the wall. Inside solid parts, the diffusion is dominant. Thus, the thermal model has to consider diffusion, convection and radiation.

2.3. Experimental conditions and characterization

Experimental conditions are presented in **Table 1**. The oven temperature is set at 1420 K. The reactor pressure, the inlet CH_4 flow and the initial porosity of carbon fleeces are equal to 0.125 bars, 1260 LNTP/h, and 0.93, respectively. The process lasts 50 h, separated into 2 cycles: a first one of 30 h, then the preform is removed and returned for a second cycle of 20 h.

Table 1. Process parameters

Parameter	Oven temperature (K)	Pressure (bar)	Fluid flow (LNTP/h)	Gas composition (%mol)	Initial porosity
Value	1420	0.125	1260	100 % CH_4	0.93

Concerning the characterization, the preform is weighed before and after 50 h of densification and an X-ray tomography, allowing quantifying homogeneity and quality of the deposition, is made after 50 h of densification. Later, it is cut into small cubes to characterize porosity more locally and quantitatively via optical microscopy and image processing. Optical microscopy characterization Fig 1 shows images collected by optical microscopy at x20 zoom. The red curve represents the evolution of porosity along the preform. The top images and curve are taken on the outer edge, while the bottom photos are taken on the inner edge. The angles noted correspond to the extinction angles of PyC. These data will be used later to calibrate the simulation model.

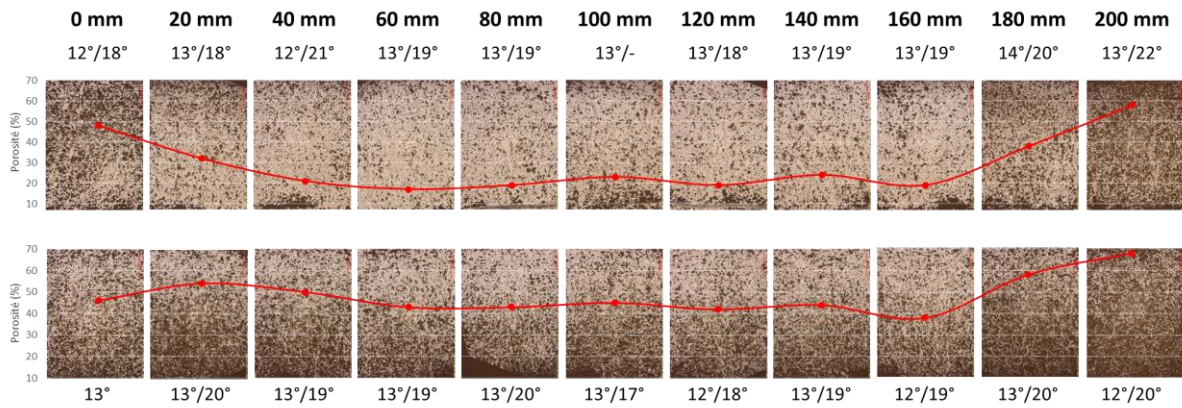


Fig 1. Optical microscopy characterization

3. Comparison between experiments and simulations

First of all, the simulation model has to be compared with experimental data. For this application, all the reactor is modeled (inlet gas, reacting part where densification proceeds and gas outlet) from hydrodynamics, kinetics, heat transfer and porosity points of view. Results allow observing velocity and temperature fields, product concentrations, and density evolution, against space and time.

Concerning the validation, the experimental final measured mass of the densified device is about 2045 g with a standard deviation of 50.5 g whereas the simulated final mass of the device is 1996 g after 50 h of densification, which validates the order of magnitude of the calculated total mass. Fig 2 shows a comparison between simulated density and experimental results obtained by X-ray tomography. In the tomography picture, the red curve corresponds to the density (qualitative results) obtained on the vertical axis described by the green line. It is possible to see that on the top of tomography and simulation (near the outlet of the densification part), the density is lower especially on the inner wall (left part of the tomography analysis). In the middle and at the bottom of the densified device, the density seems to be constant, both from simulations and tomography points of view.

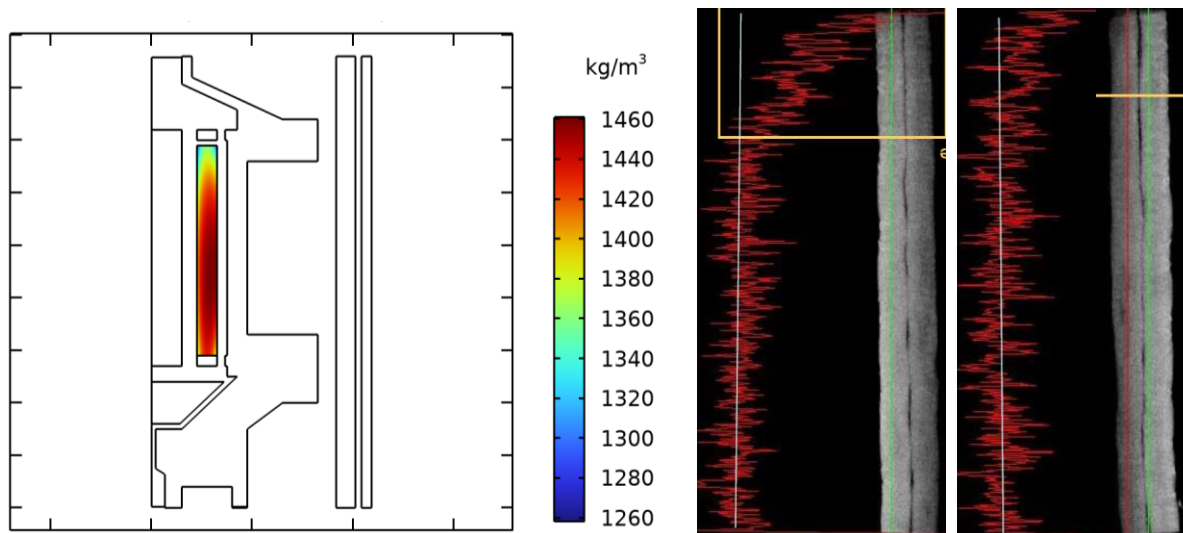


Fig 2. Comparison between X-ray tomography and simulation results

Finally, porosity measurements on Fig 3 and Fig 4 show that the simulation models PyC deposition well, both qualitatively and quantitatively. On the inner wall, the simulation seems to densify the preform a little too much, but models the trend well. This discrepancy could be explained by heat losses not taken into account by the model.

The next part deals a theoretical parametric study to find ways of optimizing the process.

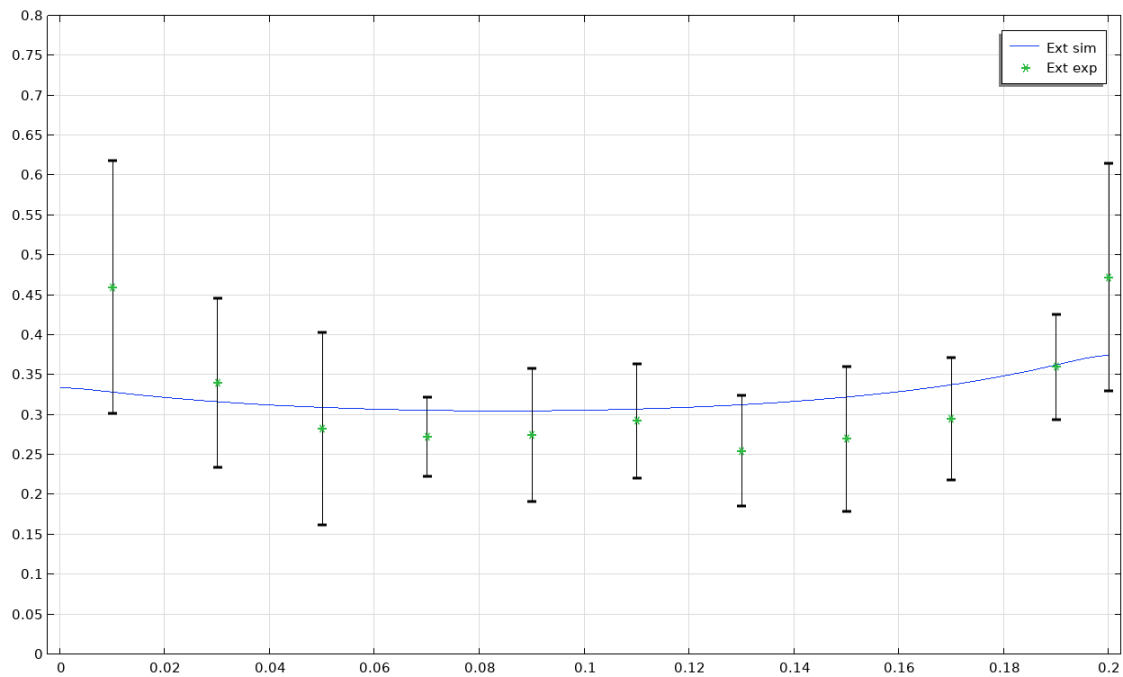


Fig 3. Comparison between simulation and optical microscopy porosity on the external wall

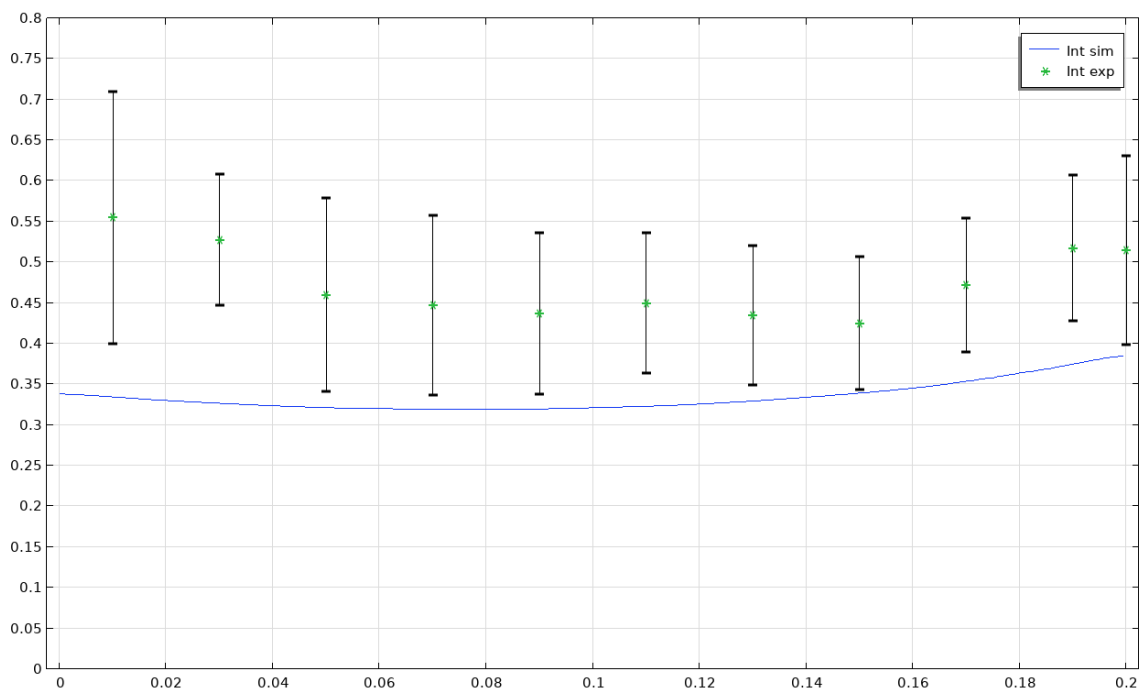


Fig 4. Comparison between simulation and optical microscopy porosity on the internal wall

4. Impact of process parameters

4.1. Impact of temperature

The influences of process parameters such as temperature, pressure, inlets flow rates or composition can be studied thanks to the simulation. For this abstract, the temperature has been chosen because it is the most important factor impacting carbon deposition. The temperature has been varied between

1300 K to 1460 K and the mass, as well as the porosity repartition, are analyzed. Fig. 2 only describes the densification zone in 2D axisymmetric view (density distributions) after 50h of densification, for isothermal temperature, and feed flow rate equivalent to those of the complete reactor.

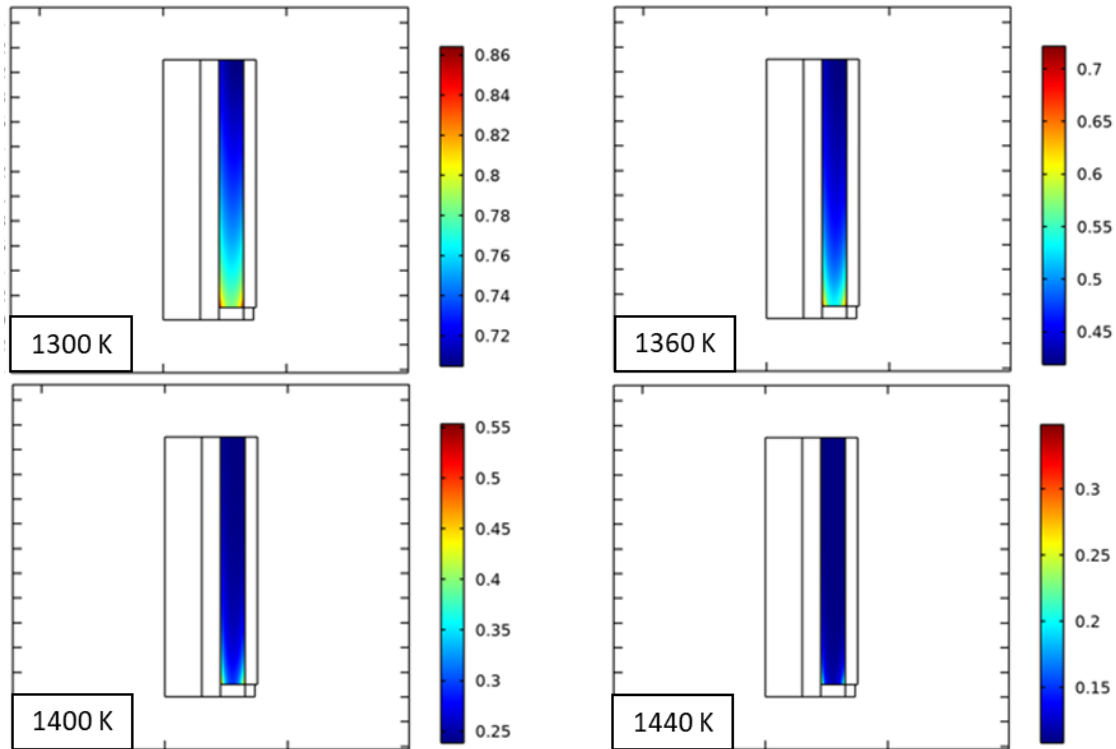


Fig 5. Density distribution at different temperatures

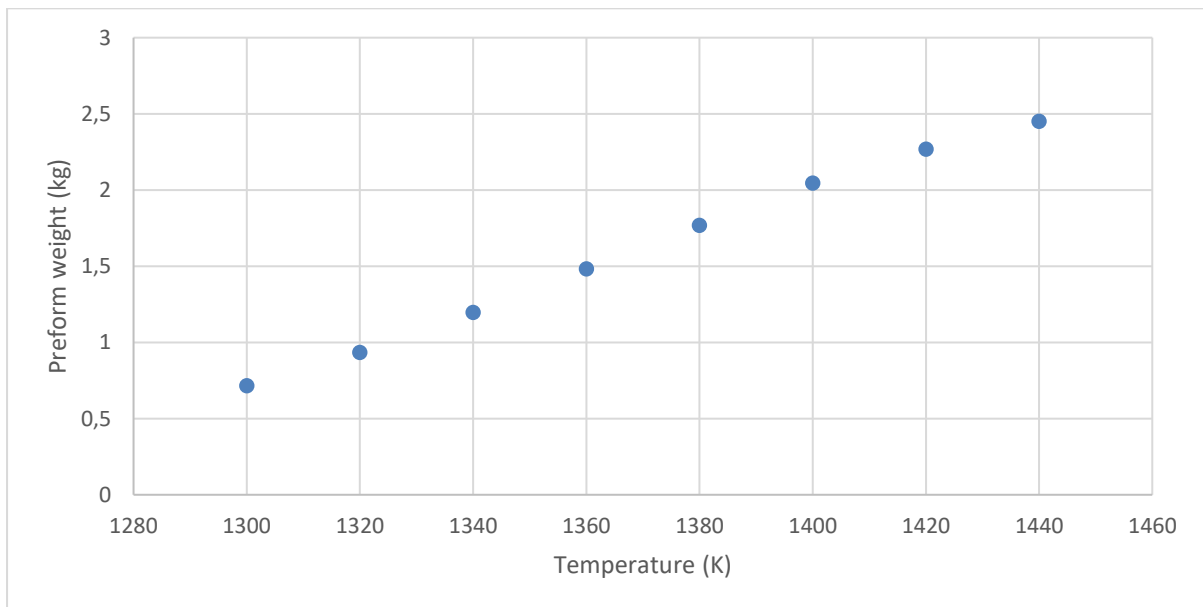


Fig 6. Mass of the preform after 50 h of densification at different temperatures

As can be seen in Fig 5, when the temperature increases, the global porosity decreases, highlighting the impact of the process temperature in the final mass of the densified product. Concerning the homogeneity, increasing temperature seems to improve the carbon distribution at the bottom of the device: the density is more homogeneous at higher temperatures. Fig 6 shows the mass of the preform

after 50 h of densification at different temperatures. The points seem to follow an affine function, showing that a small increase in temperature greatly increases the deposition. This shows that methane diffuses very well into the preform even as the temperature rises.

The influences of other process parameters, such as pressure and inlet velocities.

4.2. Impact of pressure

Pressure plays a key role in deposition speed, particularly in the methane initiation reaction that produces the methyl radical. Pressure also plays a role in the diffusion of gaseous species in the preform: too high pressure can lead to premature clogging of surface pores. Figure 7 shows that an increase in pressure does not seem to have any impact on the homogeneity of the deposit, and in particular not on surface clogging. Figure 8 shows that an increase in pressure increases the total deposit mass for a 50 h deposit. The trend appears to be logarithmic, indicating that pressure has less impact than temperature on densification.

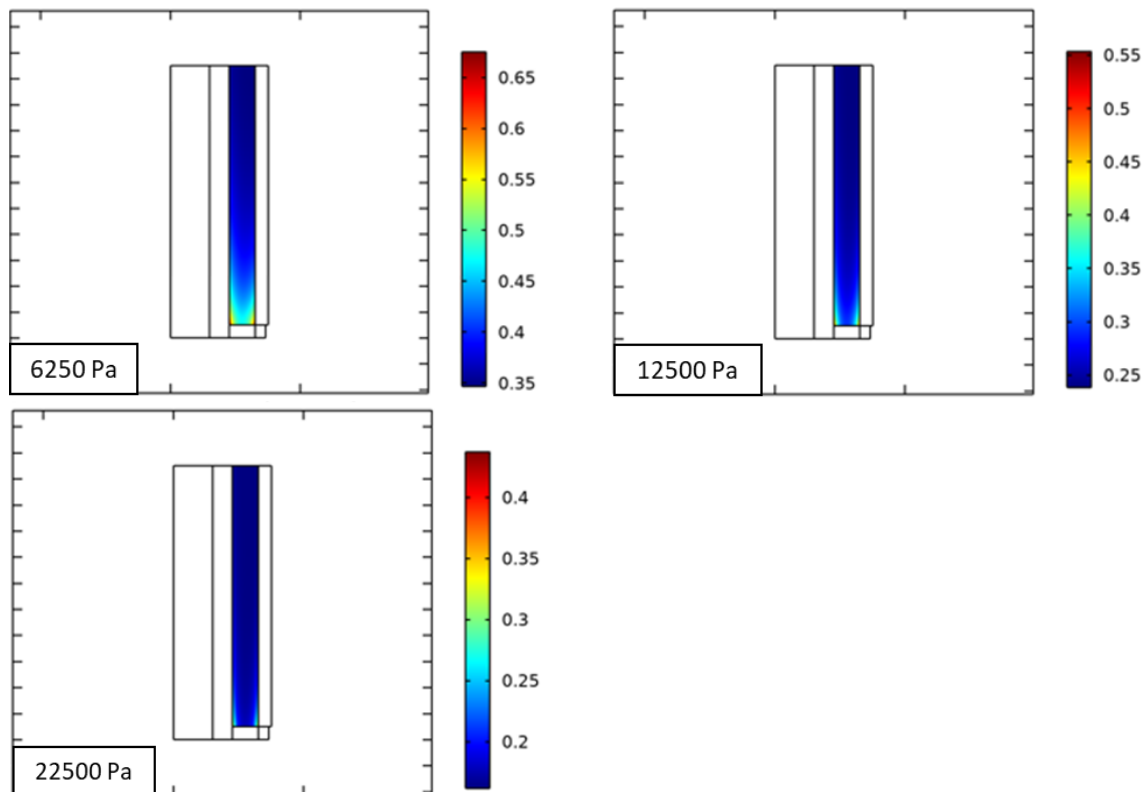


Fig 7. Density distribution at different pressures

4.3. Impact of fluid flow

Gas velocity plays a dual role: it brings in carbon that can be deposited, and it affects residence time. There will therefore be competition between these two aspects. Fig 9 shows the evolution of the final mass of the preform at 50 h at different inlet speeds. It can be seen that the mass increases with decreasing entry speed. This evolution appears linear from 1 m/s to 4.5 m/s, then slows down below 1 m/s. It would appear that an optimal velocity exists and that it lies between 0 and 0.5 m/s.

5. Conclusion

In conclusion, the complete model appears to be quantitatively close to the experimental results. Some future experimental results should improve its quality.

The parametric study highlighted the strong impact of temperature, but also of other parameters such as pressure and feed flow rate. This can serve as a basis for improving the densification of C/C composite by r-CVI process, whose results will be confirmed by future experimental trials.

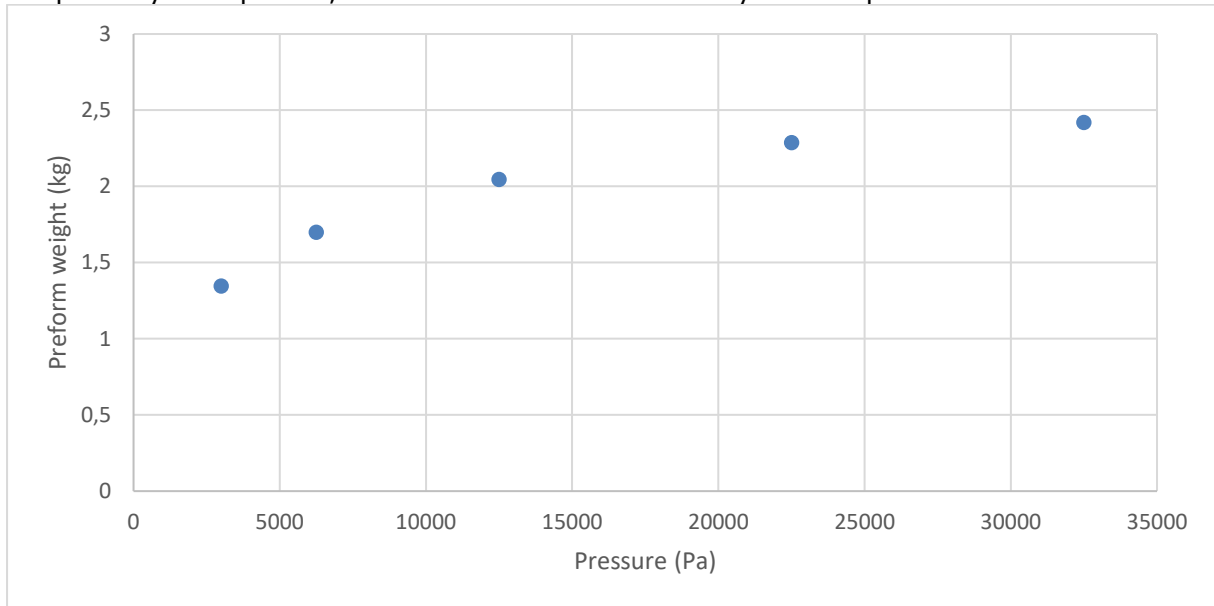


Fig 8. Mass of the preform after 50 h of densification at different pressures

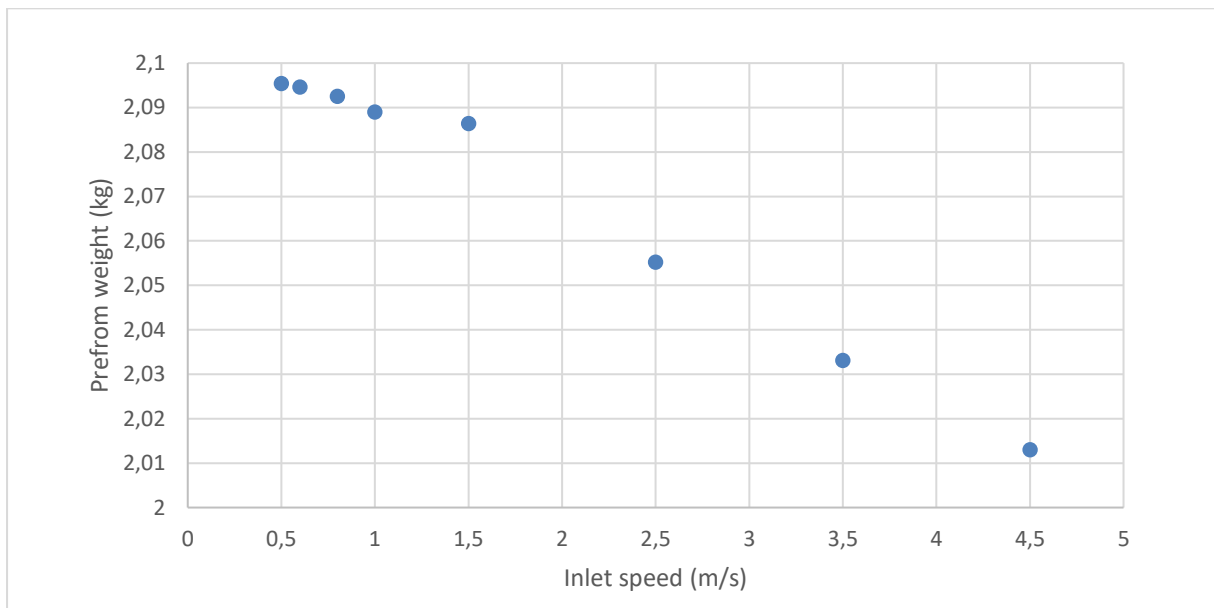


Fig 9. Mass of the preform after 50 h of densification at different gas velocities

6. References

- [1] G. L. Vignoles, Y. Aspa, et M. Quintard, « Modelling of carbon–carbon composite ablation in rocket nozzles », *Composites Science and Technology*, vol. 70, n° 9, p. 1303-1311, sept. 2010, doi: 10.1016/j.compscitech.2010.04.002.
- [2] E. Fitzer et L. M. Manocha, *Carbon Reinforcements and Carbon/Carbon Composites*. Berlin, Heidelberg: Springer Berlin Heidelberg, 1998. doi: 10.1007/978-3-642-58745-0.
- [3] A. Desenfant, « Dépôt chimique en phase vapeur (CVD) de carbure de silicium (SiC) à partir de vinyltrichlorosilane (VTS) et de méthylsilane (MS) », p. 251.
- [4] P. Delhaes, « Chemical vapor deposition and infiltration processes of carbon materials », *Carbon*, vol. 40, n° 5, p. 641-657, avr. 2002, doi: 10.1016/S0008-6223(01)00195-6.
- [5] Y. Xu et X.-T. Yan, *Chemical Vapour Deposition*. in Engineering Materials and Processes. London: Springer London, 2010. doi: 10.1007/978-1-84882-894-0.
- [6] I. Ziegler, R. Fournet, et P. M. Marquaire, « Pyrolysis of propane for CVI of pyrocarbon », *Journal of Analytical and Applied Pyrolysis*, vol. 73, n° 2, p. 212-230, juin 2005, doi: 10.1016/j.jaap.2004.12.005.
- [7] I. Ziegler, R. Fournet, et P.-M. Marquaire, « Pyrolysis of propane for CVI of pyrocarbon », *Journal of Analytical and Applied Pyrolysis*, vol. 73, n° 2, p. 231-247, juin 2005, doi: 10.1016/j.jaap.2005.03.007.
- [8] R. Lacroix, R. Fournet, I. Ziegler-Devin, et P.-M. Marquaire, « Kinetic modeling of surface reactions involved in CVI of pyrocarbon obtained by propane pyrolysis », *Carbon*, vol. 48, n° 1, p. 132-144, janv. 2010, doi: 10.1016/j.carbon.2009.08.041.